Incorporating demographic information into spawner-recruit analyses alters biological reference point estimates for a western Alaska salmon population

BENJAMIN A. STATON*
Fishery Science Department, Columbia River Inter-Tribal Fish Commission, 700 NE Multnomah St., Ste. 1200, Portland, OR 97232
School of Fisheries, Aquaculture, and Aquatic Sciences, Auburn University, 203 Swingle Hall, Auburn, AL 36849
bstaton@critfc.org

MATTHEW J. CATALANO
School of Fisheries, Aquaculture, and Aquatic Sciences, Auburn University, 203 Swingle Hall, Auburn, AL 36849
mjc0028@auburn.edu

STEVEN J. FLEISCHMAN
Division of Sport Fish, Alaska Department of Fish and Game (Retired), 333 Raspberry Rd., Anchorage, AK 99518
sjfleischman2@gmail.com

JAN OHLBERGER
School of Aquatic and Fishery Sciences, University of Washington, 1122 NE Boat St, Seattle, WA 98195
janohl@uw.edu

Keywords: spawner quality, Chinook salmon, demographic trends, state-space models, integrated models

*Corresponding Author

Abstract

Changes over time in age, sex, and length-at-age of returning Pacific salmon have been widely observed, suggesting concurrent declines in per capita reproductive output. Thus, assessment models assuming stationary reproductive output may inaccurately estimate biological reference points that inform harvest policies. We extended age-structured state-space spawner-recruit models to accommodate demographic time trends and fishery selectivity to investigate temporal changes in reference points using Kuskokwim River Chinook salmon (*Oncorhynchus tshawytscha*). We illustrate that observed demographic changes have likely reduced per capita reproductive output in an additive manner, for example, models including changes in both length-at-age and age composition showed larger declines than models incorporating only one time trend. Translated into biological reference points using a yield-per-recruit algorithm, we found escapement needed for maximum sustained catch has likely increased over time, but the magnitude further depended on size-selective harvest (i.e., larger increases for reference points based on larger mesh gillnets). Compared to traditional salmon assessments, our approach that acknowledges demographic time trends allows more complete use of available data and facilitates evaluating trade-offs among gear-specific harvest policies.

1 Introduction

Trends in demographic characteristics of Pacific salmon (*Oncorhynchus* spp.) have been widely observed throughout their range, particularly for Chinook salmon (*O. tshawytscha*). In many Chinook salmon populations, the average age and size at a given age of adult fish returning to their natal spawning grounds have declined since at least the 1970s (Ricker 1981; Bigler et al. 1996), including populations that spawn in the rivers of Alaska (Kendall and Quinn 2011; Lewis et al. 2015) and along much of the west coast of North America (Ohlberger et al. 2018; Losee et al. 2019). The causes of these widespread demographic trends are largely unknown, but hypothesized drivers include competition with other species of Pacific salmon in the ocean (Oke et al. 2020), intensifying size-selective marine mammal predation (Ohlberger et al. 2019), climate factors influencing growth rates (Xu et al. 2020), and fisheries-induced evolution (Eldridge et al. 2010). Regardless of their cause, changes in the size-at-age and age composition of spawning populations have led to pronounced declines in the mean body size of individual spawners and are of concern because they likely reduce the per capita reproductive output (e.g., fecundity) of breeders (Forbes and Peterman 1994; Ohlberger et al. 2020) and possibly that of their progeny (Hankin et al. 1993). These changes may have long-term impacts on population productivity, fishery catches, and ecosystem benefits (Oke et al. 2020). Over the past decade, return abundances of many Chinook salmon populations in Alaska have declined, concurrent with the declines in mean size and age (Dorner et al. 2018; Schindler et al. 2013; Ohlberger et al. 2016).

Spawner-recruit analyses used in the management of Pacific salmon usually do not account explicitly for changes in demographic attributes of the spawning escapement and thus assume reproductive output is homogeneous among individuals and static over time. Population reference points derived from these spawner-recruit analyses are often used to configure fishery management strategies (Clark et al. 2009), e.g., estimates of the number of spawners required to achieve maximum sustained catch (S_{MSC}; catch meaning

total numbers harvested, regardless of age, sex, or biomass). Traditional spawner-recruit analyses assume that the recruitment relationship is repeatable and stationary, i.e., that expected recruitment and its variability at a fixed number of spawners is constant over time (Walters and Martell 2004, Ch. 7). Using the number of spawners, regardless of demographic composition, as the sole predictor of recruitment may be overly simplistic if per capita reproductive output of those spawners (i.e., "escapement quality") trends over time. For example, if per capita fecundity is a function of the size, age, or sex of the average spawner, then the aforementioned trends in these characteristics could alter population productivity even if spawner abundance remains the same.

Studies on other commercially important fish species suggest that trends in population age structure can affect recruitment (Shelton et al. 2015), and that incorporating information on demographic variation can improve the estimation of biological reference points (Murawski 2001; Wang et al. 2005). For fishes in general, large females are known to contribute more to population replenishment per unit body weight than small females, due to higher reproductive investment and resulting output (Barneche et al. 2018). It is known for Chinook salmon that large females produce more and larger eggs than their smaller (younger) counterparts (Healey and Heard 1984; Beacham and Murray 1993; Forbes and Peterman 1994; Ohlberger et al. 2020). Thus, failing to account for time trends that suggest increasing rarity of the most productive individuals may lead to biases in S_{MSC} and related escapement-based quantities relevant to setting harvest policies.

These issues warrant exploration of alterations to spawner-recruit models that accommodate time trends in demography and heterogeneous reproductive output of different spawners, as suggested by an expert panel on declines of Chinook salmon in Alaska (Schindler et al. 2013). Variability in age composition has been incorporated into spawner-recruit models for Chinook salmon in Alaska as random fluctuations (e.g., Fleischman et al. 2013; Hamazaki et al. 2012; Staton et al. 2017) or with estimated time trends (Fleischman and McKinley 2013; McKinley and Fleischman 2013; Reimer and DeCovich 2020), but only

as a means to explain variability in the data and not as an explicit link to escapement quality or productivity. Size-based escapement goals have been implemented for Chinook salmon in the Kenai River (Fleischman and Reimer 2017) to address assessment limitations (i.e., uncertainties in size-based sonar species apportionment) and in southeast Alaska (Heinl et al. 2014), but in general, escapement quality concerns have rarely been translated to changes in Pacific salmon management.

In this article, we translate time trends in demographic characteristics (sex structure, age composition, and size-at-age) to annual estimates of total reproductive output of the spawning escapement, expressed as either total egg or egg mass production. Such estimates serve as useful alternative metrics of reproductive output with which to inform spawner-recruit models that consider escapement quality. Using integrated state-space models augmented by a yield-per-recruit algorithm, we present an evaluation of the effects of demographic trends on Pacific salmon population dynamics and fishery biological reference points. We apply the model to data from Chinook salmon in the Kuskokwim River, western Alaska. Because many of the age and sex composition data originated from size-selective gillnet fisheries, we were compelled to include selectivity in the model to accurately quantify changes in demographic characteristics of the population. Demographic time trends are long-term, and we do not attempt to attribute them to any cause; rather our objective is to quantify their magnitude and likely consequences for biological reference point estimates. However, incorporating size-selectivity enabled us to evaluate the effects of size-selective harvest on spawner composition and biological reference points and to provide helpful guidance on the risks and benefits of selective removal while jointly considering trending demographics.

2 Methods

2.1 Study system

The main-stem Kuskokwim River is approximately 1,500 km in length and contains a river network that drains approximately 130,000 km^2. The Kuskokwim contains the

largest subsistence fishery for Chinook salmon in the state of Alaska: an average of 65,000 Chinook salmon were harvested annually between 1995 and 2015 (range 15,000 – 104,000), composing 48% (range: 34 – 61%) of state-wide Chinook salmon subsistence harvests (Fall et al. 2018). Although limited bycatch occurs in offshore fisheries, targeted fishery harvests occur in-river during the spawning migration using drift gillnets, and have produced exploitation rates ranging from 13% (in 2017) to 74% (in 1982, 1976 – 2019 average: 40%, Larson 2020). Participants in subsistence and commercial fisheries are primarily native Alaskans, and the resource constitutes an integral part of the culture and lifestyle in the region (Wolfe and Spaeder 2009). Of the five species of anadromous Pacific salmon that return annually to the Kuskokwim River, Chinook salmon are favored by the subsistence fishery (Hamazaki 2008). Although Chinook salmon have been incidentally caught by the in-river commercial fishery, they have not been targeted since 1984 when a 6-inch (~15 cm) or less stretched mesh gillnet restriction was implemented with the intent of commercially targeting the more abundant stocks of chum (*O. keta*) and sockeye (*O. nerka*) salmon. The abundance of Chinook salmon returning to the Kuskokwim annually has oscillated on an approximately decadal scale, with the most recent peak abundance of approximately 325,000 fish in 2006 (Larson 2020). Since that time, annual Chinook runs have averaged approximately 120,000 fish between 2010 and 2019 necessitating severe restrictions to the subsistence fishery (which requires 67,200 – 109,800 Chinook salmon annually to meet basin-wide harvest needs, Shelden et al. 2016). The Chinook salmon stock is managed using a basin-wide fixed escapement goal policy of 65,000 – 120,000 fish annually, informed by a state-space spawner-recruit analysis that, as is traditional, models recruitment as a function of total spawners that escape harvest (Hamazaki et al. 2012). In order to meet this goal in recent years of below-average abundance, subsistence harvests have been limited primarily through mesh size restrictions (6-inch or less since 2014) and severely restricted fishing opportunities, especially in the lower river where the majority of the fishery is located (Staton 2018).

2.2 Analytical approach

Our approach to investigating the impacts of temporal changes in demographic attributes of the escapement on biological reference points involved multiple steps. First, we developed an extension of state-space spawner-recruit analyses (i.e., akin to those documented in Fleischman et al. 2013) to accommodate (*i*) sex structure as well as age structure, (*ii*) terms that quantify time-trending probabilities of return by age and sex, (*iii*) estimation of age/sex-based selectivity by multiple fisheries using different gears and exploitation rates, and (*iv*) the use of alternative units of reproductive output (e.g., fecundity rather than total spawners) which may also have a time-trending nature resulting from changes in female size-at-age (model described in section 2.4). Next, we fitted 12 versions of this model that differed in the assumed units of reproductive output and assumptions about whether return by age, sex, or size are time-constant or time-trending (section 2.5, Table 1). We then supplied estimates of population dynamics and demographic parameters to a yield-per-recruit algorithm (section 2.6) to estimate reference points (e.g., escapement and harvest at maximum sustained catch; S_{MSC} and H_{MSC}) grouped into specific temporal strata to quantify changes in these quantities over time.

2.3 Data sources

The data spanned observations of Chinook salmon between 1976 and 2019 – nearly all sampling was conducted by the Alaska Department of Fish and Game (ADF&G). We used four information types: (*i*) annual age/sex composition by fate (harvested in commercial fishery, harvested in subsistence fishery, or sampled from the escapement), (*ii*) annual mean size-at-age, (*iii*) annual abundance assigned to each fate, and (*iv*) allometric relationships to translate female size to expected reproductive output by age.

For sources (*i*) and (*ii*), we extracted records of individual adults sampled from commercial fishery harvests, subsistence fishery harvests, and escapement sampled from eight weir projects for which the sex, age, and length (mid-eye to tail-fork; METF, mm) were measured. Sex was determined by internal inspection for harvest-related fates and

external inspection at weir projects; age was assigned using scale samples in all cases (Froning and Liller 2019). We discarded records with missing age or sex assignments. When calculating the average METF or age/sex composition for each year and fate, we used a within-year temporally stratified design to minimize bias resulting from any potentially non-representative sampling. We grouped samples into 2-week strata and calculated the composition or mean METF by age/sex for each stratum. We then averaged the resulting strata-specific estimates, weighted by stratum size (e.g., estimated weir passage in each 2-week stratum). For weirs, we applied the stratification design to each weir separately, then averaged the results across weirs weighted by the weir-specific annual passage estimates. Some imputation for missing values in the METF data was necessary given that the uses of these data required values each year; we used a linear interpolation rule for this purpose (see Online Supplement A, Section #1).

For data source (*iii*), we extracted aggregate basin-wide annual escapement estimates, commercial harvest estimates, and subsistence harvest estimates from Larson (2020). That report documents a run reconstruction model that estimates basin-wide annual run size (non-age/sex-specific) from a host of assessment projects. Although Brooks and Deroba (2015) caution against using model output as data in subsequent analyses, Staton et al. (2017) performed an investigation on the topic in the context of Kuskokwim River Chinook salmon spawner-recruit analyses. They found that an integrated approach which embedded the run reconstruction calculations within the observation model of state-space spawner-recruit analyses provided nearly identical estimates (and simulation-estimation performance) to a more "sequential" approach which treated aggregate escapement estimates as observed data with associated observation variance. Given this finding, we constructed our model sequentially, where the estimation of these aggregate abundance quantities was performed external to the state-space model (i.e., by Larson 2020), and we fitted to them as though they were observed data.

Finally, for data source (*iv*) we required a relationship to predict year- and age-

specific reproductive output (e.g., fecundity) from female size. Although fecundity data for Kuskokwim River Chinook salmon have been collected, sampling has been highly opportunistic and primarily from size-selective fishery harvests. To avoid depending on these possibly unreliable data for our main analysis, we used samples of Canadian-origin Chinook salmon in the nearby Yukon River collected between 2008 and 2010 in Eagle, AK using multi-mesh gillnets and a more rigorous sampling design (Ohlberger et al. 2020). The data set included paired measurements of METF, egg count per female, and egg (ovary) mass per female from 140 individuals. We fitted power functions to these data to approximate the relative reproductive output of females of different ages based on observed mean METF from each year for the Kuskokwim River population. We analyzed six additional Alaska Chinook salmon fecundity data sets to assess the sensitivity of our conclusions to our choice of data set; our results regarding reference points were nearly identical regardless of which fecundity relationship we used (see Online Supplement A, Section #2).

2.4 State-space model to accommodate attributes of escapement

The state-space model we developed was based on the age-structured framework of Fleischman et al. (2013) but extended to accommodate more demographic attributes of the escapement. Specifically, we included three extensions, all of which were age/sex-structured: heterogeneous reproductive output across ages and sexes, expected probability of return by age and sex, and size-selectivity of several fisheries. We constructed the model such that time trends in these factors may be included or can be assumed to be non-existent (as in the traditional approach to salmon stock assessment). The model tracks latent (i.e., true, but partially or imperfectly unobserved) states of recruitment (R), escapement (S), and harvest (H) by fishery, all on an age/sex-structured basis in a stochastic population dynamics process model, of which the parameters are estimated from available data. Multiple formulations of the state-space model were fitted in this analysis (12 in total, see section 2.5 and Table 1). Given that these alternative models are simplified generalizations

of a full model (symbology summarized in Table 2), we present the full formulation with the subsequent section devoted to the specific treatment of demographic trends and units of reproductive output in other models.

2.4.1 *Biological process model*

Accounting of fish begins at the top-most level with the least amount of structure: total adult recruitment (R_y), indexed only by brood year indicating that it is the aggregate of all adults that ever return from brood year y, regardless of age (a) or sex (s). In the absence of process error, deterministic recruitment ($\dot{R}_y$) by brood year was:

$$\log(\dot{R}_y) = \begin{cases} \log(\dot{R}_0) & \text{if } y \leq a_{\max} \\ \log(\alpha) + \log(Z_{t=y-a_{\max}}) - \beta Z_{t=y-a_{\max}} & \text{if } y > a_{\max} \end{cases}, \quad (1)$$

where α and β are Ricker (1954) parameters, $a_{\max}$ is the maximum age of return (we used $a_{\max} = 7$ for Kuskokwim Chinook salmon), $\dot{R}_0$ is the expected recruitment in the $a_{\max}$ brood years prior to the first year of monitoring, and $Z_{t=y-a_{\max}}$ is the total annual reproductive output in calendar (i.e., observational or return year) year t and took on the value of:

$$Z_t = \sum_{s}^{n_s} \sum_{a}^{n_a} S_{t,a,s} \cdot z_{t,a,s}, \quad (2)$$

where $S_{t,a,s}$ is year-, age-, and sex-specific escapement from eq. 11 below, n_s is the number of sexes included in the model ($n_s = 2$), and n_a is the number of possible ages adults can return to spawn ($n_a = 4$). The quantity $z_{t,a,s}$ is the expected reproductive output per individual in each year, age, and sex. Traditional spawner-recruit models can be expressed by setting all elements of $z_{t,a,s}$ to 1, in which case $Z_t = S_t$. For descriptive purposes, we also calculated annual per capita reproductive output by dividing Z_t by S_t, which provided an index of reproductive output by the average spawner regardless of age or sex. We treated latent recruitment states (i.e., realized, with process error, R_y) as lognormal random variables around the deterministic $\dot{R}_y$, and included lag-1 autoregressive errors:

$$\log(R_y) \sim \mathrm{N}\left(\log(\dot{R}_y) + \omega_y, \sigma_R^2\right), \quad (3)$$
$$\omega_y = \phi\left(\log(R_{y-1}) - \log(\dot{R}_{y-1})\right),$$

where ϕ is the lag-1 autoregressive coefficient and σ_R^2 is the variance of white noise process variability. We used two separate σ_R^2 terms: one for the period where $\dot{R}_y$ was constant ($\sigma_{R_0}^2$), and one for the period that included the reproductive link in eq. 1.

For linkage to observations made on a calendar year basis, R_y must be apportioned to the year, age, and sex at which these adults make the spawning migration. We used probability vectors ($\pi_{y,a,s}$) to represent the marginal probability of return at age a by sex s and brood year y to perform this apportionment as shown in eq. 7. We chose to model return probabilities as separate sex and age processes to allow investigation of time trends separately with respect to these two demographic quantities. We used linear models to capture time trends in probabilities of return by sex and age to enable expressing time-constant or time-varying demographic quantities – had we used a stochastic expression such as a white noise model (e.g., as in Fleischman et al. 2013) or a random walk model, the random deviates would attempt to follow the trend and prevent us from evaluating the consequences of failing to account for certain trends. We modeled the probability that recruits R_y would return as female (ψ_y, regardless of age) as a logit-linear model:

$$\mathrm{logit}(\psi_y) = \delta_0 + \delta_1 y, \quad (4)$$

where δ_1 is an additive effect of year on the log odds of returning as a female. A time-constant version can be expressed by fixing δ_1 at zero, in which case δ_0 is the log odds of female return averaged across all brood years. We apportioned total recruitment to each sex:

$$R_{y,s} = \begin{cases} R_y\psi_y & \text{if } s = \text{female} \\ R_y(1-\psi_y) & \text{if } s = \text{male} \end{cases}. \quad (5)$$

We obtained sex-specific return-at-age probability vectors ($\pi_{y,a,s}$) for each brood year using

a baseline-category logit model (Agresti 2012, Ch. 7):

$$\eta_{y,a,s} = \begin{cases} \gamma_{0,a,s} + \gamma_{1,a,s} y & \text{if } a \leq n_a - 1 \\ 0 & \text{if } a = n_a \end{cases} \tag{6}$$

$$\pi_{y,a,s} = \frac{e^{\eta_{y,a,s}}}{\sum_{b=1}^{n_a} e^{\eta_{y,b,s}}}$$

where $\eta_{y,a,s}$ represents the log ratio of return probabilities at age a and age n_a in year y for sex s. As in the binary logit-linear model in eq. 4, the $\gamma_{1,a,s}$ coefficients can be fixed at zero to express time-constant probability vectors $\pi_{y,a,s}$. Regardless, the $\gamma_{0,n_a,s}$ and $\gamma_{1,n_a,s}$ coefficients were always fixed at zero because we used the last return age as the baseline group in eq. 6. We then apportioned recruits to abundance ($N_{t,a,s}$) in the appropriate calendar year, age, and sex in which they would return to spawn and be observed:

$$N_{t,a,s} = R_{y=t+n_a-a,s} \cdot \pi_{y=t+n_a-a,a,s} \tag{7}$$

The year indexing maps the brood year index y in which the adults of age a returning in calendar year t were spawned (see Online Supplement A, Section #3 for more details).

2.4.2 *Fishery process model*

Total abundance (age/sex-specific or otherwise) is rarely ever observed (i.e., censused). Instead, fish are counted (or estimated) according to their fate, either as harvest or as escapement and a subset is sampled for age and sex characteristics. Due to size-selective fishery harvest, individuals of different ages and sexes have unequal probabilities of capture by fisheries using different gillnet mesh sizes and exploitation rates, which could result in the age/sex composition signal differing among fates. To build an observation model that can accommodate this among-fate variability, we further apportioned the modeled abundance $N_{t,a,s}$ according to fate by age and sex using a size-selectivity function embedded within the state-space model. Both the commercial and subsistence fisheries have primarily used drift gillnets to harvest salmon and both have experienced an unrestricted mesh period (typically 7.5- or 8-inch [~20cm] stretched mesh) and a restricted mesh period (6-inch mesh

or less). We modeled size-selection using the Pearson gillnet selectivity model (Bromaghin 2005), which has the advantage of expressing selectivity as a function of the ratio between fish length to mesh perimeter (RLM). This allowed a single set of parameters to explain size-selectivity regardless of the mesh size used by each fishery each year. The Pearson gillnet selectivity model has the form:

$$V(x) = \left(1 + \frac{\lambda^2}{4\theta^2}\right)^{\theta} \times \left(1 + \frac{\left(x - \frac{\sigma\lambda}{2\theta} - \tau\right)^2}{\sigma^2}\right) \times \exp\left(-\lambda\left(\tan^{-1}\left(\frac{x - \frac{\sigma\lambda}{2\theta} - \tau}{\sigma}\right) + \tan^{-1}\left(\frac{\lambda}{2\theta}\right)\right)\right), \quad (8)$$

as presented by Bromaghin (2005), where x is the fish size:mesh perimeter ratio and τ, σ, θ, and λ are parameters controlling the location and shape of the selectivity function subject to the constraints $\sigma > 0$ and $\theta > 0$. We used estimates of τ, σ, θ, and λ from a lower Kuskokwim River multi-mesh test fishery project (operated for species apportionment of sonar counts, methods described in Birchfield and Smith 2019) to formulate weak priors on these parameters. We used independent normal prior distributions (zero-truncated where necessary) with mean equal to those provided by ADF&G (N. Smith, personal communication) but with variance equal to $(\mathrm{SE} \times 10)^2$ to reduce the information content of the prior (Table 3). We compared the marginal posterior and prior density functions for these parameters to verify that minimal information was introduced. More vague uniform priors resulted in excessively poor mixing that was remedied to some extent by these weak priors.

We standardized the Pearson selectivity function such that one age/sex class was fully selected by each mesh size (m) each year:

$$v_{t,a,s,m} = \frac{V(\mathrm{RLM}_{t,a,s,m})}{\max\left(V\left(\mathrm{RLM}_{t,1:n_a,1:n_s,m}\right)\right)}, \quad (9)$$

which allowed for the annual intensity of fishing pressure to be identifiably expressed as the fishing mortality of the fully selected age/sex class. We calculated the input $\text{RLM}_{t,a,s,m}$ values using the mean METF by age, sex, and year from the escapement data set assuming two mesh sizes: 8-inches and 6-inches. We chose to use escapement METF data because sampling can be assumed to be non-size-selective, this source had the longest and most complete data set, and any missing values had already been imputed for populating $z_{t,a,s}$ (reproductive output see section 2.5 and Online Supplement A, Section #1 therein for more details).

We modeled harvest by the commercial and subsistence fisheries separately, given that total harvest estimates were available for each and they have different management and monitoring histories. Each fishery had an estimated fishing mortality of the fully selected age/sex class ($F_{\text{sub},t}$ and $F_{\text{com},t}$), allowing us to model harvest on a fishery/year/age/sex-specific basis by using the appropriate value of m (mesh size index):

$$
\begin{aligned}
F_{\text{tot},t,a,s} &= F_{\text{sub},t} v_{t,a,s,[\text{sub}_t]} + F_{\text{com},t} v_{t,a,s,[\text{com}_t]}, \\
H_{\text{sub},t,a,s} &= N_{t,a,s} \frac{F_{\text{sub},t} v_{t,a,s,[\text{sub}_t]}}{F_{\text{tot},t,a,s}} \left(1 - e^{-F_{\text{tot},t,a,s}}\right), \\
H_{\text{com},t,a,s} &= N_{t,a,s} \frac{F_{\text{com},t} v_{t,a,s,[\text{com}_t]}}{F_{\text{tot},t,a,s}} \left(1 - e^{-F_{\text{tot},t,a,s}}\right),
\end{aligned}
\tag{10}
$$

where $v_{t,a,s,[\text{sub},t]}$ denotes age/sex-specific selectivity of mesh size type m used by the subsistence fishery in year t and likewise for $v_{t,a,s,[\text{com},t]}$ and the commercial fishery. We then obtained age/sex-structured escapement ($S_{t,a,s}$) as:

$$
S_{t,a,s} = N_{t,a,s} - H_{\text{sub},t,a,s} - H_{\text{com},t,a,s}. \tag{11}
$$

As is common in salmon stock assessment models, we did not include terms for natural sources of post-harvest mortality (e.g., predation) in eqs. 10 or 11 since very little, if any, data exist to inform them and the time period between passing through the primary harvest areas in the lower main-stem Kuskokwim River and reaching the spawning grounds in the tributaries is relatively short (i.e., several weeks or months).

2.4.3 *Observation model*

We summarized the values of $H_{\text{sub},t,a,s}$, $H_{\text{com},t,a,s}$, and $S_{t,a,s}$ to fit to the observed data. The observed abundance of escapement and harvest each year were available as aggregate estimates, not partitioned into age or sex. Thus for fitting to (e.g.,) $S_{obs,t}$, we calculated the expectation S_t as $\sum_s^{n_s} \sum_a^{n_a} S_{t,a,s}$ and used it in a lognormal likelihood with assumed known observation variance $\sigma^2_{S,t}$. We used the same likelihood expression for aggregate harvest from each fishery separately. Similarly, we obtained modeled age/sex composition from (e.g.,) $S_{t,a,s}$ by calculating the proportion in each unique age/sex category (j, of which there were eight elements: four ages by two sexes) each year t and used it as the expectation in a multinomial likelihood, linking the expected fate-specific age/sex composition to their observed frequencies (e.g., $x_{S,t,j}$). We used the same likelihood expression for age/sex composition from each fishery.

The observation variance terms for abundance states (e.g., $\sigma^2_{S,t}$) were informed using the estimated coefficient of variation (CV) provided by ADF&G: ($\sigma^2 = \log\left((\text{CV}/100)^2 + 1\right)$), which characterizes assessment uncertainty. Observation CVs were generally higher for escapement [average: 12%, range: 5 – 27%; Larson (2020)] than for subsistence harvest (average: 5%, range: 1 – 10%; e.g., Shelden et al. 2016) or commercial harvest (all year CV = 2%, estimated annually via mandatory trip tickets, Hamazaki et al. 2012). Although the CVs may seem low (e.g., for aggregate escapement), they were estimated by the same models that produced the estimates we used as data and were the best expressions of observation uncertainty available to us, and we preferred to use these estimated values instead of applying arbitrary rules that would increase their value. See Online Supplement A, Section #4 for details on how we obtained effective sample size (set lower than observed sample size, Maunder 2011) for multinomial likelihoods and a sensitivity analysis to the specific method we used.

2.5 Alternative assumptions for state-space model

2.5.1 Unit of reproductive output

We assessed three sets of alternative assumptions for the unit of reproductive output for an average spawner of age a and sex s returning in calendar year t. Traditional Pacific salmon spawner-recruit analyses assume that all spawners contribute equally to production of progeny, thus expressing the α (productivity) parameter in terms of maximum recruits-per-spawner, regardless of age or sex. Our state-space model can accommodate this assumption by setting all elements of $z_{t,a,s}$ equal to 1, which results in $Z_t = S_t$ in eq. 2. However, larger (older) females generally produce more eggs (Healey and Heard 1984; Ohlberger et al. 2020), and it is thus reasonable to expect that they should produce more progeny than females of younger, smaller age classes. We used the aforementioned fecundity data from the Yukon River (2008 – 2010) to fit a power function of the form $\text{eggs} = a \cdot \text{METF}^b$, then calculated "expected" fecundity of the average (Kuskokwim) female spawner in each year, by age, using mean METF from Kuskokwim River escapement sampling (see Online Supplement A, Section #2 for a sensitivity analysis using other Chinook salmon fecundity data sets). We used the expected eggs per female year and age to populate the elements of $z_{t,a,s}$ for females while setting male elements to zero. This assumes that male abundance is sufficient to ensure all (or a constant fraction of) eggs are fertilized and that there is no survival benefit for eggs fertilized by older males. Further, not only do larger females produce more eggs but their eggs also tend to be larger (Beacham and Murray 1993; Ohlberger et al. 2020), implying a possible survival benefit to the progeny resulting from more resources at the embryo and alevin stages (Forbes and Peterman 1994). Thus, we fitted another power function with total egg mass as the response variable (from the same Yukon River data set) and used its predictions to populate the $z_{t,a,s}$ elements for a third assumption about how relative reproductive output varies with age and year. Note that all future uses of egg number and egg mass in the context of Kuskokwim Chinook salmon refer to these expectations derived using Kuskokwim River METF data in Yukon

River allometric relationships. We denote these models as N-* (all $z_{t,a,s}$ elements equal to one), E-* ($z_{t,a,s}$ based on eggs per female), and EM-* ($z_{t,a,s}$) based on total egg mass per female; Table 1).

2.5.2 Included time trends

We designed the state-space model specifically to investigate the influence of trends in sex composition, age composition, and length-at-age on biological reference points: by comparing the output from models that include these trends to those that do not (Table 1), we were able to quantify these influences. We expressed time-trending probability of return-by-sex by estimating δ_1 from eq. 4 and expressed the time-constant version by fixing δ_1 at zero. Likewise, we expressed time-trending probabilities of return-at-age by estimating the $\gamma_{1,a,s}$ terms from eq. 6 and fixing their values at zero for the time-constant version. To incorporate time-varying length-at-age (and thus expected reproductive output for models E-* and EM-*), we used annual values of $z_{t,a,s}$ obtained from the Yukon River power functions and Kuskokwim River METF data in eq. 2, and implemented the time-constant version by averaging $z_{t,a,s}$ across years for each age a and sex s. All models included selectivity terms following eqs. 8, 9, and 10 in which $\text{RLM}_{t,a,s,m}$ varied each year depending on the value of METF for each age and sex. We denote models with none of these time trends (regardless of reproductive unit) by *-0, return-at-age trends by *-A, return-by-sex trend by *-S, and length-at-age trends by *-L; we denote models with more than one trend included by, e.g., *-ASL (Table 1).

2.6 Equilibrium calculations

Traditional calculations (Scheuerell 2016) and approximations (Hilborn 1985) for S_{MSC} and H_{MSC} and other equilibrium quantities assume all spawning individuals contribute equally to future generations. Because some of our models relaxed this assumption and because the probability of escaping harvest by age/sex was a function of fishing mortality and mesh size, a yield-per-recruit approach was required to obtain estimates of these biological reference points. To find S_{MSC} and H_{MSC}, we constructed an optimization algorithm that

iteratively searched for the fishing mortality of the fully selected age/sex class ($F_{\max}$) such that total harvest (regardless of age or sex) was maximized, and the corresponding value of escapement at that $F_{\max}$ level was taken as S_{MSC}, also regardless of age or sex. To evaluate whether our findings were general to other biological reference points, we used the same approach to calculate the spawner abundance ($S_{R_{\mathrm{MAX}}}$) and harvest ($H_{R_{\mathrm{MAX}}}$) at maximum recruitment by setting total recruitment as the objective to maximize instead of catch. We conducted the calculations that follow externally to the fitting of state-space models, but for each posterior sample from each model to propagate parameter uncertainty. Further, we summarized state-space model output into temporal strata: all years (1976 – 2019), the first 10 years (1976 – 1985), and the last 10 years (2010 – 2019) for equilibrium calculations. To isolate the temporal effects of demographic trends from size-selective harvest, we evaluated a scenario that was not size-selective (all v terms set to 1) in addition to the 6-inch and 8-inch mesh size scenarios. Required outputs from state-space models for yield-per-recruit analyses were α, ϕ, σ_R^2, β, $\bar{\pi}_{i,j}$, $\bar{v}_{i,j,m}$, and $\bar{z}_{i,j}$; the bar denotes averages over some time period (indexed by i) and j represents a unique age/sex class.

We calculated reproductive output-per-recruit (z_{PR}) under fishing mortality $F_{\max}$ for a fishery using mesh m as a function of the age/sex class-specific reproductive output ($\bar{z}_{i,j}$) weighted by the probability of returning by age/sex ($\bar{\pi}_{i,j}$) and the probability of escaping harvest ($1 - U_{i,j}$):

$$z_{\mathrm{PR},i,m} = \sum_j (1 - U_{i,j,m}) \bar{z}_{i,j} \bar{\pi}_{i,j}, \tag{12}$$

where $U_{i,j,m} = 1 - e^{-F_{\max} v_{i,j,m}}$. Following Walters and Martell (2004), we then calculated total equilibrium recruitment as:

$$R_{\mathrm{eq},i,m} = \frac{\log(\alpha_c z_{\mathrm{PR},i,m})}{\beta z_{\mathrm{PR},i,m}}, \tag{13}$$

We used the corrected version of α (α_c) to adjust for auto-correlated lognormal process errors, where:

$$\alpha_c = e^{\log(\alpha)+\sigma_R^2/\left(2(1-\phi^2)\right)}. \tag{14}$$

Once the scale of the equilibrium population fished at $F_{\max}$ was obtained from eq. 13, we calculated the age/sex structured abundance, harvest, and escapement:

$$\begin{aligned} N_{\text{eq},i,j,m} &= R_{\text{eq},i,m}\bar{\pi}_{i,j}, \\ H_{\text{eq},i,j,m} &= N_{\text{eq},i,m}U_{i,j,m}, \\ S_{\text{eq},i,j,m} &= N_{\text{eq},i,m}(1-U_{i,j,m}), \end{aligned} \tag{15}$$

and calculated totals for harvest and escapement by summing over ages and sexes:

$$\begin{aligned} H_{\text{eq},i,m} &= \sum_j H_{\text{eq},i,j,m}, \\ S_{\text{eq},i,m} &= \sum_j S_{\text{eq},i,j,m}. \end{aligned} \tag{16}$$

$H_{\text{eq},i,m}$ was treated as the objective value to maximize via iterative numerical search on the quantity $F_{\max}$ for S_{MSC} calculations and the objective value was $R_{\text{eq},i,m}$ for $S_{R_{\text{MAX}}}$ calculations.

2.7 Computation and model fit

State-space model parameters were estimated with Markov chain Monte Carlo (MCMC) methods implemented in JAGS (Plummer 2003) invoked through R (R Core Team 2019) using the package "jagsUI" (Kellner 2018). We selected prior distributions to be as minimally informative as possible, while preventing the sampler from considering biologically implausible or invalid areas of the parameter space (Table 3). Long MCMC chains were necessary to ensure convergence (checked visually and using the $\hat{R}$ statistic, Brooks and Gelman 1998) and adequate information content for posterior inference (checked using the effective MCMC sample size). We used posterior predictive checks to verify model adequacy for the data (Kéry 2010; Gelman et al. 2014) and the Wantanabe-Akaike information criterion (WAIC) as a measure of model parsimony (Hooten and Hobbs 2015).

We summarized all posterior distributions using the median and 95% equal-tailed

credible intervals unless otherwise stated. In all cases where a quantity was derived from estimated parameters, (e.g., S_{MSC} derived from α and β), we performed the calculation for each sample from the joint posterior for that model, then summarized the resulting marginal posterior. All code for data preparation, JAGS models, making use of High Performance Computing resources, and output summarization is documented in Staton (2020).

No models displayed egregious lack of MCMC convergence or inadequacy for the data, though posterior predictive checks did suggest aggregate escapement estimates with assumed-known lognormal observation variance were over-dispersed relative to model fitted values (more details in Online Supplement A, Section #5 therein and model-specific Online Supplements B – I). WAIC tended to favor models that included trends in the probabilities of returning by age and sex – suggesting patterns in the data justified the additional model complexity (Table 1). Among models that used fecundity as the unit of reproductive output, the model with time trends for age and sex was the top model, but the model also including length time trends came in close second (Table 1); we think the similarity is due to these two models having the same number of parameters and the lack of a length-based likelihood function like those for age and sex composition. Regardless of this finding that some models had more statistical support than others, we present inferences from multiple models to illustrate the contrast among different assumptions about how time trends in demography affect population productivity and biological reference points.

3 Results

3.1 Fishery selectivity

The estimated selectivity function from all models indicated a dome-shaped pattern with fish of intermediate size relative to the perimeter of the mesh (RLM) being those most selected (Figure 1). The curve was nearly identical for all models, regardless of the assumed unit of reproductive output or included time trends. Fish with RLM values equal to 1.88

were estimated to be most selected, (~760 mm and ~570 mm METF for 8-inch and 6-inch mesh, respectively). Across ages, the consequence of this estimated function for both sexes was a dome-shaped pattern for 8-inch mesh (Figure 2a), and a declining pattern for 6-inch mesh (Figure 2b). Due to changes in mean length-at-age over time, we would not expect the relative selectivity of different ages and sexes to be static, and indeed when stratified into early (first 10 years; 1976 – 1985) and late (last 10 years; 2010 – 2019) time blocks, we found this to be the case. The most pronounced temporal shifts in selectivity were for age-5 and age-6 males fished with 8-inch mesh: the model suggested increasing relative selectivity for age-6 and decreasing relative selectivity for age-5 in recent years (Figure 2a).

Selectivity parameters were estimable because (*i*) we fitted to fate-specific age/sex composition data, (*ii*) these were weighted by the aggregate abundance of fish in each fate, and (*iii*) the two fisheries did not use the same mesh size each year. From 1976 – 1983, both fisheries used mostly 8-inch mesh and showed similar fitted age and sex composition, namely that they were made up of fewer age-4 and more age-5 fish than the escapement (Figure 3). Starting in 1984, the commercial fishery was restricted to using 6-inch mesh while the subsistence fishery continued to use 8-inch mesh, and at this point the composition of the two fisheries experienced a pronounced separation: the commercial fishery was comprised of more age-4 males than either the escapement or subsistence composition time series and the subsistence fishery was comprised of more age-5 and age-6 females (especially after 2000) and age-6 males than either the escapement or commercial harvest (Figure 3). Starting in 2014, the subsistence fishery was also restricted to 6-inch mesh, at which point the subsistence and commercial fisheries again showed similar composition time series. Although the patterns displayed in Figure 3 are posterior medians, they agreed well with the raw age and sex composition data from scale counts sampled throughout the basin (Online Supplements B – I; Figure 2 in each document).

3.2 Estimated demographic trends

3.2.1 Return-by-sex

For models with δ_1 fixed at zero (thus assuming probability of return-by-sex is time-constant), the posterior median probability of returning as a female from any brood year was 0.34 (0.32 – 0.36; all intervals in parentheses are 95% credible limits). For models that freely estimated δ_1 (thus allowing time-trending probability of return-by-sex), the posterior probability ranged from 0.41 (0.36 – 0.46) in the first tracked brood year (1969) to 0.29 (0.26 – 0.32) in the last brood year (2015), and these values were nearly identical among models that varied in other aspects. The median value of the δ_1 coefficient was -0.012 (-0.018 – -0.005), meaning that in each brood year, recruits were 98.9% (98.2 – 99.5%) times as likely to return as female than in the previous brood year.

3.2.2 Return-at-age

For models that allowed return-at-age probabilities to vary with respect to brood year, clear patterns were identified in which returning at younger ages has become more likely over time for both sexes (Figure 4). Among females, the probability of returning at age-4 continued to be as low as in the beginning of the time series (less than 5% of all female recruits), however the probability of returning at age-5 has increased, while returning at age-6 and age-7 has declined (Figure 4). For example, in the first brood year, the posterior median probability of returning at age-6 for females was 0.76 (0.69 – 0.82) compared to 0.59 (0.52 – 0.66) in the last brood year, whereas for age-5 this change went from 0.12 (0.08 – 0.17) to 0.36 (0.3 – 0.43). For males, the largest temporal changes occurred for age-4 and age-6, with the former becoming approximately twice as common and the latter becoming approximately half as common over the time frame included in the model (Figure 4).

3.2.3 Assumed reproductive output

Both alternative measures (egg number and egg mass) indicated that reproductive output increases sharply and disproportionally with fish size. The egg number per female spawner relationship obtained from the Yukon River population sampled at Eagle, AK was 9.3 $\times$

$10^{-4} \cdot \text{METF}^{2.36}$ and for egg mass (g) per female spawner it was $8.7 \times 10^{-12} \cdot \text{METF}^{4.83}$ (Figure 5) – these relationships enabled modeling how relative reproductive output from individual female spawners may have changed over time with observed trends in female length-at-return by age. The egg mass relationship suggested a steeper increase in relative reproductive output with increasing length (age) than the egg number relationship. For example, using the average METF-at-age in the first 10 years of the data set in the equations above, age-5 females produced 69% as many eggs as an age-7 female, but only 46% of the egg mass (Figure 5a). In comparing the first 10 years to the last 10 years, moderate changes in female length-at-return (5-10% depending on age) resulted in comparatively large changes in reproductive output (Figure 5b), especially when egg mass rather than egg number was considered. For example, average METF for age-6 females has decreased by 7% (first 10 years versus last 10 years), but this is expected to have resulted in a 17% reduction in the number of eggs produced by age-6 females, and a 31% reduction in total egg mass (Figure 5b). Females of all ages showed reductions in mean size and expected fecundity measures except for age-4 females, which have increased in mean length by 5% – though considering they make up less than 5% of all female recruits (Figure 4), these increases are unlikely to offset the decreases for the other ages.

3.2.4 Per capita reproductive output

We found that per capita reproductive output has likely changed over time as a result of these demographic changes, but that the extent depended on which trends were included in the model (Figure 6), and only for models that used heterogeneous reproductive output across ages (models N-0 and N-ASL assumed per capita reproductive output was time invariant and constant across individuals). When only one trend was included in the model at a time (models E-L, E-A, and E-S), the model with a trend included for return-by-sex (model E-S) exhibited the largest change in per capita reproductive output: the early period was approximately 15% higher and the later period was approximately 15% lower than the mean across all years (21% overall decline; Figure 6). For two-trend models,

the model with both sex-at-return and length-at-return (model E-SL) exhibited the largest per capita shift (31% overall), but it was similar in magnitude to that suggested by model E-AS (29% overall). The change over time was larger still for the three-trend models and was more exaggerated for the model treating egg mass as the unit of reproductive output (EM-ASL) rather than egg count (E-ASL). Model EM-ASL suggested that the average spawner in the early third of the time series produced 30% more reproductive output than the average of the whole time series, and that spawners in the later third produced approximately 25% less reproductive output (49% decline overall). Models using eggs or fewer trends than model EM-ASL exhibited smaller declines in per capita reproductive output: models E-ASL, E-AL, E-L, and E-A showed overall declines of 39%, 23%, 15%, and 11%, respectively.

3.3 Equilibrium values

Models that expressed reproductive output in terms of fish units (models N-0 and N-ASL, collectively denoted N-*) were insensitive to the mesh size, time period, and incorporated trends in equilibrium calculations (Figure 7). This is because N-* models assumed all fish contributed equally to producing the next generation, i.e., age/sex composition and selective harvest had no bearing on per capita reproductive output. However, when either eggs (models denoted E-*) or egg mass (EM-*) were used, we found sensitivity in the equilibrium values of S_{MSC} and H_{MSC}, which depended strongly on fishery selectivity, considered time period, and included demographic trends. The equilibrium quantities associated with maximum recruitment rather than maximum catch ($S_{R_{\mathrm{MAX}}}$ and $H_{R_{\mathrm{MAX}}}$) showed similar patterns as those described below (Online Supplement A, Section #6).

3.3.1 Large mesh gillnets

Assuming large (8-inch) mesh would be used exclusively by the fishery, models E-0 and EM-0 suggested a median increase of approximately 30% in S_{MSC} from model N-0 (90,000 versus 69,000 total spawners) considering all years of demographic information (Figure 7a). Incorporating trends in age- (A), sex- (S), and length-at-return (L) resulted in similar

563 percent increases ranging from 25% (model E-A) to 42% (model EM-ASL). The time period
564 of information used in equilibrium calculations had a large effect on these changes, with
565 the earlier period having values of median S_{MSC} closer to the N-0 model, and the late
566 period having larger values. Further, the extent of this time dependency was influenced by
567 which trends were accounted for: models with only one trend (models E-A, E-S, and E-L)
568 were less sensitive to the considered time period than the models that accounted all three
569 trends simultaneously (models E-ASL and EM-ASL), and there was not a strong tendency
570 for any one trend (A, S, or L) to be driving this pattern. Notably, the assumed reproductive
571 unit did not have a major impact on the inference (Figure 7a), i.e., the scale and shift over
572 time in S_{MSC} was similar for models E-ASL (86% temporal increase) and EM-ASL (100%
573 temporal increase).

574 Increases in the spawning abundance needed to maintain a maximum sustainable
575 catch were accompanied by decreases in the level of H_{MSC} achieved. This pattern was
576 driven mostly by increased S_{MSC} and not reduced recruitment when fished at MSC. Models
577 E-* and EM-* showed a range (across models) of 10-17% declines in median H_{MSC} relative
578 to model N-0 when all years of demographic information were considered, and 15-45%
579 declines when only the most recent 10 years were considered (Figure 7b).

580 *3.3.2 Smaller mesh gillnets*

581 Unlike for the large mesh scenario, median S_{MSC} was suggested to be lower for the E-* and
582 EM-* models than for the N-* models by a range (across models) of 15 – 30% when all years
583 were considered (Figure 7e), which resulted in increases of H_{MSC} that ranged between 10 –
584 17% across models (Figure 7f). This resulted from the ability to exert a higher exploitation
585 rate on young males, which are abundant yet were assumed to contribute no reproductive
586 output and are mostly invulnerable to capture by the larger mesh. Maximizing catch with
587 small mesh under models E-* and EM-* involved an exploitation rate of approximately 80%
588 for the entire population (70% for females and 85% for males overall), but for age-4 males
589 the rate was 97% and 85% for age-5 males, which collectively make up approximately 50%

of all returning adults. When fished at these levels, the yield-per-recruit model suggested that the post-harvest sex composition would switch from being male dominated (~65% males) to being approximately evenly split between sexes. As for the larger mesh scenario, there was still a tendency to need to allow more total spawners (29% increase for model E-ASL) and lower H_{MSC} (12% decrease for model E-ASL) when considering the most recent 10 years relative to the earliest 10 years, but the difference was far less exaggerated than in the larger mesh scenario.

3.3.3 Non-selective mesh gillnets

In comparison to the large mesh scenario, the analysis involving a hypothetical gear combination that could exert no size-selectivity suggested less pronounced effects of demographic changes on S_{MSC} (Figure 7c) and H_{MSC} (Figure 7d). Though it would be difficult to construct a non-selective gillnet, this alternative provides a way to isolate the effects of trending demography from those of fishery selectivity. Note that, in the absence of size-selectivity, the E-0 and EM-0 models provided nearly the same estimates of S_{MSC} and H_{MSC} as the N-0 model, indicating that, for this stock, the choice of reproductive unit alone had little effect on the reference points. However, when the demographic trends were included (models E-ASL and EM-ASL), reference point estimates (and their changes over time) were intermediate between those from the large and small mesh scenarios.

4 Discussion

We have illustrated that the estimation of biological reference points is sensitive to assumptions regarding the reproductive contribution of different spawners (i.e., fecundity rather than simple spawner units) and which demographic changes are acknowledged in spawner-recruit analysis. Most importantly, we found that S_{MSC} increased and H_{MSC} decreased when we incorporated demographic time trends based on empirical field data (fewer females, younger age-at-return, and smaller size-at-age). Further, we showed a strong dependence of both the scale of S_{MSC} and H_{MSC} and the magnitude of temporal changes on the selectivity of the gear used to harvest the population – our analysis sug-

gests fisheries using smaller mesh sizes require fewer escaping fish because they target smaller and less productive individuals. Although these results make intuitive sense, the state-space approach we used enabled their rigorous quantification based on robust statistical methods and transparent assumptions.

Concerns about declining Pacific salmon escapement quality are often expressed by fisheries managers and stakeholders, however, they are rarely explicitly accounted for in stock assessments or management strategies. A notable exception is the example of the "big fish goal" for Kenai River Chinook salmon (Fleischman and Reimer 2017), which although it was motivated by sonar assessment limitations (i.e., overlap in length distributions among species make size-based species apportionment difficult for smaller salmon), may have benefits for long-term population productivity. We think the discrepancy between concern and action is a result of two main factors: (*i*) it is not always clear how to leverage available data to formulate a defensible stock assessment model that accounts for escapement quality and (*ii*) lack of a transparent way to develop and implement management strategies based on escapement quality rather than total number of fish harvested or escaped. To our knowledge, ours is the first Pacific salmon spawner-recruit model to explicitly link estimated demographic trends from observed data to population production feedback. By developing the yield-per-recruit model to provide estimates of management reference points, we made a first attempt at translating demographic changes into reference points relevant to fishery managers.

By incorporating demographic time trends into the assessment model, we identified evidence for declines in per capita reproductive output for Kuskokwim River Chinook salmon. Expressed as total annual egg production divided by total spawner abundance, we estimated an average decline in per capita reproductive output of 39% when all demographic time trends were included in the model. Calculating per capita reproductive output this way accounts for changes in fecundity at a given age weighted by changes in female prevalence and age composition, thus is a more comprehensive expression than

644 quantifying changes in any one demographic quantity in isolation of the others. It is
645 likely that a change in per capita reproductive output of this magnitude is a contributor
646 to the observed non-stationarity in productivity and declines in abundance in recent
647 years (Dorner et al. 2018; Schindler et al. 2013; Ohlberger et al. 2016). Although we
648 performed our analysis with only the Kuskokwim River Chinook salmon population,
649 it is not unique in exhibiting demographic time trends (Lewis et al. 2015; Ohlberger
650 et al. 2018; Oke et al. 2020) and we expect that this is a much broader issue than solely
651 the Kuskokwim River population or even western Alaska as a whole. However, our
652 focus was to investigate sensitivity of assessment models and biological reference point
653 estimates to the incorporation of demographic time trends, not to quantify evidence for the
654 relative contribution of different causal factors for observed non-stationary productivity.
655 Investigations wishing to address this latter topic must consider demographic time trends
656 alongside a suite of other hypothesized mechanisms such as climate forcing, inter-specific
657 interactions, and habitat changes.

658 In addition to the incorporation of demographic trends that feed back into population
659 dynamics, the other aspect of our model that is not generally included in Pacific salmon
660 stock assessments is the selectivity function. With the addition of only four parameters
661 plus length-at-age observations, our model was able to accommodate multiple sampling
662 processes that differed in selectivity. The more realistic observation model enabled more
663 complete use of the available data and made it possible to obtain a representation of
664 the unharvested run age composition. This separation of latent versus external factors
665 highlights a distinct advantage of our analytical approach over other studies that analyze
666 demographic trend data in isolation of fisheries management or sampling regimes (e.g.,
667 Lewis et al. 2015; Ohlberger et al. 2018). Furthermore, incorporation of the selectivity
668 function enabled quantification of size-selective harvest effects on suggested reference
669 points. We identified a clear trade-off between gear restrictions and the value of S_{MSC}
670 that suggested fewer fish need to escape the fishery if a smaller mesh size is used. This

was largely due to the selective removal of younger, less productive spawners by smaller mesh (Figure 2b). This finding implies that escapement goal ranges that acknowledge escapement quality should perhaps be on a "sliding scale" depending on the selectivity of the gear used by the fishery. Further, although we designed our equilibrium calculations to estimate biological reference points for a single fishery (i.e., one $F_{\max}$ and mesh size combination), reference points based on multiple simultaneous fisheries could be obtained if the algorithm was supplied with a proportional allocation and the mesh size used by each fishery (e.g., Goethel et al. 2018).

Our equilibrium approach to estimating biological reference points was useful in that it translated observed demographic trends into changes in measures from which harvest policies are commonly developed. However, this approach is admittedly not likely the optimal way to evaluate candidate escapement levels that take into account escapement quality concerns. Salmon fisheries management has multiple objectives (e.g., inter-annual stability in catch may be more relevant than its long-term maximization), and the equilibrium approach we used only maximized one objective at a time (total catch or total recruitment) and it did not acknowledge inter-annual variability in harvest outcomes. Future analyses could express utility in terms of value measures other than numbers of fish harvested, such as total biomass harvested, total eggs deposited, or age diversity in the spawning escapement in an attempt to better characterize attainment of harvest- and conservation-based objectives. Further, our assumption that males contribute no reproductive output made sense for model fitting (e.g., allowed α to represent maximum expected recruits-per-egg), but produced some unrealistic results when used to calculate reference points (i.e., inflated exploitation rates, particularly for young males). We think the ideal way to evaluate harvest policies (e.g., escapement goals) in this context would be to use stochastic simulation. Using this approach, one would sample from the joint posterior from our state-space models, simulate the population forward through time under a range of candidate escapement goals and mesh sizes, and calculate performance metrics that

698 better-encompass the breadth of objectives relevant to managers and stakeholders. In this
699 case, it would be possible to address some of the weaknesses of our equilibrium approach
700 (e.g., incorporating inter-annual variability, assigning male spawners some reproductive
701 value, and evaluating more objectives).

702 Our approach required some noteworthy assumptions to arrive at our results. First,
703 in calculating biological reference points, we made important assumptions about the
704 reproductive utility of males. Specifically, we assumed that total reproductive output is
705 limited by females and that male abundance is always sufficient to fertilize all eggs (or
706 at least a time-constant fraction of them). Overall we believe this assumption is valid,
707 however the small mesh equilibrium scenario did suggest that when fished at MSC,
708 the sex composition of the escapement would shift close to 50% females (relative to the
709 unfished composition of ~35%) – which may reduce the validity of this assumption if the
710 population was ever fished hard enough to maximize sustained catch. Second, our annual
711 fecundity predictions were not directly measured but rather were expanded from length
712 measurements. Thus, we assumed that the allometric egg number/mass relationships
713 were time-constant, i.e., that on average, a female of a given size produced the same
714 number and mass of eggs in every year from 1976 to 2015. If factors have selectively
715 pressured females to become more or less fecund at a given size, then our estimates of how
716 reference points have changed would be biased. The limited availability of fecundity data
717 prevented us from evaluating this assumption quantitatively, but given its importance
718 we suggest that fecundity relationships be quantified with greater temporal regularity.
719 Third, similar to the previous caveat, we assumed that the expected maximum survival
720 from egg to recruit (α) is time-constant – violations in this assumption would also render
721 our estimates incorrect. Fourth, we assumed that non-retention mortality from small
722 mesh gillnets is negligible, i.e., larger fish that interact with but are not captured by small
723 mesh gillnets are not injured to an extent that would prevent successful spawning. Non-
724 retention mortality has been shown to be potentially important, for example, Baker and

Schindler (2009) estimated that sockeye salmon in Bristol Bay with gillnet injuries had pre-spawn mortality rates of 8-100%, depending on the severity of injury and the assumed threshold for stream residence time for successful spawning. If gillnet injury is a major factor affecting spawning success in Kuskokwim Chinook salmon, then our estimates of S_{MSC} for the small mesh scenario would be underestimated. Fifth, our treatment of age/sex composition data assumed that no biases in age or sex assignment exist. In general, based on the sampling methods used to collect the data we used, we are confident this assumption is valid. External sex assignment is most difficult early in the upstream migration, before fish display external cues of sexual dimorphism. Fish sampled during this part of the migration were examined internally because they were harvested. For fish sampled at weir locations, however, sex assignment bias is possible. If this bias is strongly size-dependent, then it is possible that our sex composition/trend is incorrect. For example, if small females are frequently assigned as males, then their increased prevalence over time could be perceived as declining female composition. Sixth, by freely exchanging reproductive units between numbers of spawners, numbers of eggs, and egg mass, we made simplifying assumptions about the mechanisms that underlie density-independent and density-dependent processes. For example, density-dependent survival probably operates both within individual redds (reflecting competition among progeny) and among redds (reflecting competition among spawners); thus there may be important trade-offs between small numbers of large females and large numbers of small females that we have not accounted for in this work. Finally, our use of egg mass as the unit of reproduction assumes that fish from larger eggs survive better to adulthood than fish from smaller eggs, if this is not indeed true, then inferences from the EM-* models would be identical to inferences from the E-* models.

5 Conclusions

Salmon stock assessments are most often expressed in terms of adult recruits being produced by adult spawners, which make important assumptions about the relative value

of each spawner to producing the next generation. In the absence of demographic trends that would reduce per capita reproductive output, these assumptions should be valid. However, time trends in return-by-age/sex and size-at-age have been widely observed for Chinook salmon, leading to concerns about long-term population productivity if left unaddressed. The alterations we made to the traditional recruit-per-spawner approach suggest that accounting for demographic attributes of the escapement alters the interpretation of the available data and changes estimates of biological reference points. Namely, we illustrated that since the average fish is likely less fecund now than in the past, more spawners are also likely required to produce the same number of eggs and surviving recruits. Importantly, through incorporation of the selectivity function in equilibrium calculations to derive biological reference points, we showed that at high exploitation rates that would maximize sustained harvest, fishing gear may play a central role in controlling per capita reproductive output of fish surviving the fishery. This result suggests that management targets (e.g., escapement goals) should perhaps be adjusted based on which gear is used (i.e., higher escapement necessary when large mesh is used). Surely other factors, environmental and anthropogenic, unaccounted for by our analysis, influence the survival of progeny post-spawning, but here we identified gear-specific escapement levels as a potential mechanism for managers to explicitly address escapement quality concerns. We advise that future work with Kuskokwim River Chinook salmon harvest policies use estimates of population dynamics parameters from our models to build stochastic evaluations of candidate escapement levels and mesh sizes that acknowledge changes in escapement quality. We believe more salmon stock assessment models should move in this direction of incorporating demographic attributes, and our approach should serve as a useful example and starting point for practitioners with a desire to formulate similar models for other specific cases.

Acknowledgments

We are grateful for the extensive efforts exerted by the Alaska Department of Fish and Game in collection and curation of the long and rich data time series that made our analysis possible. We thank J. Harding and J. Boersma for providing unpublished fecundity data sets to inform estimates of relative reproductive contribution for relationships used in sensitivity analyses. We thank C. Cunningham, G. Decossas, H. Hamazaki, Z. Liller, D. Schindler, N. Smith and two journal-assigned reviewers for helpful feedback on previous versions of this work that greatly improved its presentation. This work was completed in part with resources provided by the Auburn University Hopper Cluster, which facilitated fitting such a large number of complex models using MCMC. Authors B.S. and M.C. were funded in part by AYKSSI when much of our early work was conducted and author J.O. was funded in part by the NPRB. The findings and statements made herein are those solely of the authors, and do not necessarily represent the views of any organization, governmental or otherwise.

References

Agresti, A. 2012. *Categorical Data Analysis*. Wiley Series in Probability and Statistics. Wiley, 3 edition.

Baker, M. R. and Schindler, D. E. 2009. Unaccounted mortality in salmon fisheries: non-retention in gillnets and effects on estimates of spawners. *Journal of Applied Ecology*, 46(4):752–761.

Barneche, D. R., Robertson, D. R., White, C. R., and Marshall, D. J. 2018. Fish reproductive-energy output increases disproportionately with body size. *Science*, 360(6389):642–645.

Beacham, T. D. and Murray, C. B. 1993. Fecundity and egg size variation in North American Pacific salmon (*Oncorhynchus*). *Journal of Fish Biology*, 42(4):485–508.

Bigler, B. S., Welch, D. W., and Helle, J. H. 1996. A review of size trends among North Pacific salmon (*Oncorhynchus* spp.). *Canadian Journal of Fisheries and Aquatic Sciences*, 53(2):455–465.

Birchfield, K. O. and Smith, N. J. 2019. Estimated salmon abundance in the Kuskokwim River using sonar, 2017. Fishery Data Series 19-27, Alaska Department of Fish and Game, Anchorage, AK. Available at: http://www.adfg.alaska.gov/FedAidPDFs/FDS19-27.pdf [last accessed 12/20/2020].

Bromaghin, J. F. 2005. A versatile net selectivity model, with application to Pacific salmon and freshwater species of the Yukon River, Alaska. *Fisheries Research*, 74(1-3):157–168.

Brooks, E. N. and Deroba, J. J. 2015. When "data" are not data: the pitfalls of post hoc analyses that use stock assessment model output. *Canadian Journal of Fisheries and Aquatic Sciences*, 72(4):634–641.

Brooks, S. P. and Gelman, A. 1998. General methods for monitoring convergence of iterative simulations. *Journal of Computational and Graphical Statistics*, 7(4):434.

Clark, R. A., Bernard, D. R., and Fleischman, S. J. 2009. Stock-recruitment analysis for escapement goal development: a case study of Pacific salmon in Alaska. In Krueger, C. C. and Zimmerman, C. E., editors, *Pacific Salmon: Ecology and Management of Western Alaska's Populations*, American Fisheries Society Symposium 70, pages 743–758, Bethesda, MD.

Dorner, B., Catalano, M. J., and Peterman, R. M. 2018. Spatial and temporal patterns of covariation in productivity of Chinook salmon populations of the northeastern Pacific Ocean. *Canadian Journal of Fisheries and Aquatic Sciences*, 75(7):1082–1095.

Eldridge, W. H., Hard, J. J., and Naish, K. A. 2010. Simulating fishery-induced evolution in Chinook salmon: the role of gear, location, and genetic correlation among traits. *Ecological Applications*, 20(7):1936–1948.

Fall, J. A., Godduhn, A., Halas, G., Hutchinson-Scarbrough, L., Jones, B., Mikow, E., Sill, L., Trainor, A., Wiita, A., and Lemons, T. 2018. Alaska subsistence and personal use salmon fisheries 2015 annual report. Technical Paper 440, Alaska Department of Fish and Game, Anchorage, AK. Available at: http://www.adfg.alaska.gov/techpap/TP440.pdf [last accessed 2/20/2019].

Fleischman, S. J., Catalano, M. J., Clark, R. A., and Bernard, D. R. 2013. An age-structured state-space stock-recruit model for Pacific salmon (*Oncorhynchus* spp.). *Canadian Journal of Fisheries and Aquatic Sciences*, 70(3):401–414.

Fleischman, S. J. and McKinley, T. R. 2013. Run reconstruction, spawner-recruit analysis, and escapement goal recommendation for late-run Chinook salmon in the Kenai River. Fishery Manuscript Series 13-02, Alaska Department of Fish and Game, Anchorage, AK. Available at: http://www.adfg.alaska.gov/FedAidpdfs/FMS13-02.pdf [last accessed 12/20/2020].

Fleischman, S. J. and Reimer, A. M. 2017. Spawner-recruit analyses and escapement goal recommen-

dations for Kenai River Chinook salmon. Fishery Manuscript Series 17-02, Alaska Department of Fish and Game, Anchorage, AK. Available at: http://www.adfg.alaska.gov/FedAidPDFs/FMS17-02.pdf [last accessed 12/20/2020].

Forbes, L. S. and Peterman, R. M. 1994. Simple size-structured models of recruitment and harvest in Pacific salmon (*Oncorhynchus* spp.). *Canadian Journal of Fisheries and Aquatic Sciences*, 51(3):603–616.

Froning, K. E. and Liller, Z. W. 2019. Salmon age, sex, and length catalog for the Kuskokwim Area, 2016. Regional Information Report 3A19-03, Alaska Department of Fish and Game, Anchorage, AK. Available at: http://www.adfg.alaska.gov/FedAidPDFs/RIR.3A.2019.03.pdf [last accessed 12/20/2020].

Gelman, A., Carlin, J. B., Stern, H. S., Dunson, D. B., Vehtari, A., and Rubin, D. B. 2014. *Bayesian Data Analysis*. CRC Press, Boca Raton, 3 edition.

Goethel, D. R., Smith, M. W., Cass-Calay, S. L., and Porch, C. E. 2018. Establishing stock status determination criteria for fisheries with high discards and uncertain recruitment. *North American Journal of Fisheries Management*, 38(1):120–139.

Hamazaki, T. 2008. "When people argue about fish, the fish disappear." Fishery closure "windows" scheduling as a means of changing the Chinook salmon subsistence fishery pattern: is it an effective tool? *Fisheries*, 33(10):495–501.

Hamazaki, T., Evenson, M. J., Fleischman, S. J., and Schaberg, K. L. 2012. Spawner-recruit analysis and escapement goal recommendation for Chinook salmon in the Kuskokwim River drainage. Fishery Manuscript Series 12-08, Alaska Department of Fish and Game, Anchorage, AK. Available at: http://www.adfg.alaska.gov/FedAidPDFs/FMS12-08.pdf [last accessed 12/20/2020].

Hankin, D. G., Nicholas, J. W., and Downey, T. W. 1993. Evidence for inheritance of age of maturity in Chinook Salmon (*Oncorhynchus tshawytscha*). *Canadian Journal of Fisheries and Aquatic Sciences*, 50(2):347–358.

Healey, M. C. and Heard, W. R. 1984. Inter- and intra-population variation in the fecundity of Chinook salmon (*Oncorhynchus tshawytscha*) and its relevance to life history theory. *Canadian Journal of Fisheries and Aquatic Sciences*, 41(3):476–483.

Heinl, S., Jones, III, E., Piston, A., Richards, P., and Shaul., L. 2014. Review of salmon escapement goals in Southeast Alaska. Fishery Manuscript Series 14-07, Alaska Department of Fish and Game, Anchorage, AK. Available at: http://www.adfg.alaska.gov/fedaidPDFs/FMS14-07.pdf [last accessed 12/20/2020].

Hilborn, R. 1985. Simplified calculation of optimum spawning stock size from Ricker's stock recruitment curve. *Canadian Journal of Fisheries and Aquatic Sciences*, 42(11):1833–1834.

Hooten, M. B. and Hobbs, N. T. 2015. A guide to Bayesian model selection for ecologists. *Ecological Monographs*, 85(1):3–28.

Kellner, K. 2018. *jagsUI: A Wrapper Around 'rjags' to Streamline 'JAGS' Analyses*. R package version 1.5.0.

Kendall, N. W. and Quinn, T. P. 2011. Length and age trends of Chinook salmon in the Nushagak River, Alaska, related to commercial and recreational fishery selection and exploitation. *Transactions of the American Fisheries Society*, 140(3):611–622.

Kéry, M. 2010. *Introduction to WinBUGS for ecologists: a Bayesian approach to regression, ANOVA, mixed models, and related analyses*. Elsevier/Academic Press, Burlington, Massachusetts.

Larson, S. 2020. 2019 Kuskokwim River Chinook salmon run reconstruction and 2020 forecast. Regional Information Report 3A20-02, Alaska Department of Fish and Game, Anchorage, AK. Available at: http://www.adfg.alaska.gov/FedAidPDFs/RIR.3A.2020.02.pdf [last accessed 12/20/2020].

Lewis, B., Grant, W. S., Brenner, R. E., and Hamazaki, T. 2015. Changes in size and age of Chinook salmon *Oncorhynchus tshawytscha* returning to Alaska. *PLOS ONE*, 10(6):e0130184.

Losee, J. P., Kendall, N. W., and Dufault, A. 2019. Changing salmon: an analysis of body mass, abundance, survival, and productivity trends across 45 years in Puget Sound. *Fish and Fisheries*, 20(5):934–951.

Maunder, M. N. 2011. Review and evaluation of likelihood functions for composition data in stock-assessment models: Estimating the effective sample size. *Fisheries Research*, 109(2-3):311–319.

McKinley, T. R. and Fleischman, S. J. 2013. Run reconstruction, spawner-recruit analysis, and escapement goal recommendation for early-run Chinook salmon in the Kenai River. Fishery Manuscript Series 13-03, Alaska Department of Fish and Game, Anchorage, AK. Available at: http://www.adfg.alaska.gov/FedAidpdfs/FMS13-03.pdf [last accessed 12/20/2020].

Murawski, S. 2001. Impacts of demographic variation in spawning characteristics on reference points for fishery management. *ICES Journal of Marine Science*, 58(5):1002–1014.

Ohlberger, J., Scheuerell, M. D., and Schindler, D. E. 2016. Population coherence and environmental impacts across spatial scales: a case study of Chinook salmon. *Ecosphere*, 7(4).

Ohlberger, J., Schindler, D. E., Brown, R. J., Harding, J. M. S., Adkison, M. D., Munro, A. R., Horstmann, L., and Spaeder, J. 2020. The reproductive value of large females: consequences of shifts in demographic structure for population reproductive potential in Chinook salmon. *Canadian Journal of Fisheries and Aquatic Sciences*, 77(8):1292–1301.

Ohlberger, J., Schindler, D. E., Ward, E. J., Walsworth, T. E., and Essington, T. E. 2019. Resurgence of an apex marine predator and the decline in prey body size. *Proceedings of the National Academy of Sciences*, 116(52):26682–26689.

Ohlberger, J., Ward, E. J., Schindler, D. E., and Lewis, B. 2018. Demographic changes in Chinook salmon across the Northeast Pacific Ocean. *Fish and Fisheries*, 19(3):533–546.

Oke, K. B., Cunningham, C. J., Westley, P. A. H., Baskett, M. L., Carlson, S. M., Clark, J., Hendry, A. P., Karatayev, V. A., Kendall, N. W., Kibele, J., Kindsvater, H. K., Kobayashi, K. M., Lewis, B., Munch, S., Reynolds, J. D., Vick, G. K., and Palkovacs, E. P. 2020. Recent declines in salmon body size impact ecosystems and fisheries. *Nature Communications*, 11(1).

Plummer, M. 2003. JAGS: A program for analysis of Bayesian graphical models using Gibbs sampling. *3rd International Workshop on Distributed Statistical Computing (DSC 2003); Vienna, Austria*, 124.

R Core Team 2019. *R: A Language and Environment for Statistical Computing*. R Foundation for Statistical Computing, Vienna, Austria.

Reimer, A. M. and DeCovich, N. A. 2020. Susitna River Chinook salmon run reconstrution and escapement goal analysis. Fishery Manuscript Series 20-01, Alaska Department of Fish and Game, Anchorage, AK. Available at: http://www.adfg.alaska.gov/FedAidpdfs/FMS20-01.pdf [last accessed 12/20/2020].

Ricker, W. E. 1954. Stock and recruitment. *Journal of the Fisheries Research Board of Canada*, 11(5):559–623.

Ricker, W. E. 1981. Changes in the average size and average age of Pacific salmon. *Canadian Journal of Fisheries and Aquatic Sciences*, 38(12):1636–1656.

Scheuerell, M. D. 2016. An explicit solution for calculating optimum spawning stock size from Ricker's stock recruitment model. *PeerJ*, 4:e1623.

Schindler, D., Krueger, C., Bisson, P., Bradford, M., Clark, B., Conitz, J., Howard, K., Jones, M., Murphy, J., Myers, K., Scheuerell, M., Volk, E., and Winton, J. 2013. Arctic-Yukon-Kuskokwim Chinook salmon research action plan: evidence of decline of Chinook salmon populations and recommendations for future research. Report prepared for AYK Sustainable Salmon Initiative, AYK SSI Chinook Salmon Expert Panel. Available at: http://www.aykssi.org/wp-content/uploads/AYK-SSI-Chinook-Salmon-Action-Plan-83013.pdf [last accessed 12/20/2020].

Shelden, C. A., Hamazaki, T., Horne-Brine, M., and Roczicka, G. 2016. Subsistence salmon harvests in the Kuskokwim Area, 2015. Fishery Data Series 16-55, Alaska Department of Fish and Game, Anchorage, AK. Available at: http://www.adfg.alaska.gov/FedAidPDFs/FDS16-55.pdf [last accessed 12/20/2020].

Shelton, A. O., Hutchings, J. A., Waples, R. S., Keith, D. M., Akçakaya, H. R., and Dulvy, N. K. 2015. Maternal age effects on Atlantic cod recruitment and implications for future population trajectories. *ICES Journal of Marine Science*, 72(6):1769–1778.

Staton, B. A. 2018. In-season harvest and effort estimates for 2018 Kuskokwim River subsistence salmon fisheries during block openers. Project summary report, Yukon Delta National Wildlife Refuge, U.S. Fish and Wildlife Service, Bethel, AK. Available at: https://www.fws.gov/uploadedFiles/2018KuskokwimRiverSalmonSubsistenceHarvestReport.pdf [last accessed 12/20/2020].

Staton, B. A. 2020. bstaton1/esc-qual-ms-analysis: Final release (v1.0). GitHub repository housing code and data to replicate analyses available at: https://doi.org/10.5281/zenodo.4382757.

Staton, B. A., Catalano, M. J., and Fleischman, S. J. 2017. From sequential to integrated Bayesian analyses: exploring the continuum with a Pacific salmon spawner-recruit model. *Fisheries Research*, 186:237–247.

Walters, C. J. and Martell, S. J. D. 2004. *Fisheries Ecology and Management*. Princeton University Press.

Wang, S.-P., Sun, C.-L., Punt, A. E., and Yeh, S.-Z. 2005. Evaluation of a sex-specific age-structured assessment method for the swordfish, *Xiphias gladius*, in the North Pacific Ocean. *Fisheries Research*, 73(1-2):79–97.

Wolfe, R. J. and Spaeder, J. 2009. People and salmon of the Yukon and Kuskokwim drainages and Norton Sound in Alaska: Fishery harvests, culture change, and local knowledge system. In Krueger, C. C. and Zimmerman, C. E., editors, *Pacific Salmon: Ecology and Management of Western Alaska's Populations*, American Fisheries Society Symposium 70, pages 349–379, Bethesda, MD.

Xu, Y., Decker, A. S., Parken, C. K., Ritchie, L. M., Patterson, D. A., and Fu, C. 2020. Climate effects on size-at-age and growth rate of Chinook salmon (*Oncorhynchus tshawytscha*) in the Fraser River, Canada. *Fisheries Oceanography*, 29(5):381–395.

TABLE 1. Summary of state-space models fitted for this study showing the notation for how models are referenced and results of WAIC calculations. Cells with ■ indicate that particular trend was included in the model, those with □ indicate the demographic quantity was time-constant. Inclusion/exclusion of trends and alternative units of reproductive output are described in section 2.5. Supplements B – I show detailed model output from select models, including convergence summaries, model fit, posterior predictive checks, and model code. ΔWAIC values were calculated relative to the lowest value within each reproductive unit type.

		Demographic Trends				
Rep. Unit	**Model**	**Age**	**Sex**	**Length**	**Supplement**	**ΔWAIC**
Spawners	N-0	□	□	□	B	106.1
	N-ASL	■	■	■		0.0
Egg Count	E-0	□	□	□	C	104.1
	E-A	■	□	□	D	10.5
	E-S	□	■	□	E	90.9
	E-L	□	□	■	F	104.5
	E-AS	■	■	□	G	0.0
	E-AL	■	□	■		11.0
	E-SL	□	■	■		91.8
	E-ASL	■	■	■	H	0.6
Egg Mass	EM-0	□	□	□		103.5
	EM-ASL	■	■	■	I	0.0

TABLE 2. Symbology used in the presentation of the state-space model.

Symbol	Description	Eqs.
Dimensional Constants		
n_t	Number of calendar years included in the model	
n_y	Number of brood years included in the model	
n_s	Number of sexes of return	
n_a	Number of ages of return	
$a_{\min}$, $a_{\max}$	Minimum and maximum age of return, respectively	
Indices		
y, t	Brood and calendar year, respectively	
a, s	Age and sex, respectively	
j	Unique age/sex class	
m	Mesh size	
i	Time block	
Parameters		
α	Ricker productivity parameter	1,14
β	Ricker capacity parameter	1,13
ϕ	Lag-1 autoregressive coefficient	3,14
σ_R^2	White noise recruitment process variance	3,14
δ_0, δ_1	Logit-scale coefficients for sex-at-return	4
ψ_y	Probability a recruit from brood year y is female	4,5
$\gamma_{0,a,s}$, $\gamma_{1,a,s}$	Baseline logit-scale coefficients for age-at-return	6
$\pi_{y,a,s}$	Year- and sex-specific probability of return-at-age	6,7
τ, σ, θ, λ	Parameters of the Pearson gillnet selectivity function	8
$v_{t,a,s,m}$	Selectivity in year t for age a and sex s using mesh m	9,10
$F_{\text{com},t}$	Fishing mortality of the commercial fishery in year t	10
$F_{\text{sub},t}$	Fishing mortality of the subsistence fishery in year t	10
States		
$\dot{R}_y$	Expected recruitment for brood year y	1,3
$\dot{R}_0$	Expected recruitment for brood years without spawner-link	1
R_y	Realized recruitment for brood year y	3,5,7
$N_{t,a,s}$	Run abundance in calendar year t of age a and sex s	7,10
$H_{\text{com},t,a,s}$	Commerical harvest in calendar year t of age a and sex s	10
$H_{\text{sub},t,a,s}$	Subsistence harvest in calendar year t of age a and sex s	10
$S_{t,a,s}$	Escapement in calendar year t of age a and sex s	2,11
Z_t	Total reproductive output in calendar year t	1,2
Assumed Known Quantities		
$z_{t,a,s}$	Reproductive output of a spawner in year t	2
$S_{obs,t}$, $H_{\text{com},t}$, $H_{\text{sub},t}$	Observed (estimated) aggregate escapement, commerical harvest, and subsistence harvest in year t	
$\sigma^2_{S,t}$, $\sigma^2_{\text{com},t}$, $\sigma^2_{\text{sub},t}$	Observation variances for aggregate escapement, commercial harvest, and subsistence harvest in year t	
$x_{S,t,j}$, $x_{\text{com},t,j}$, $x_{\text{sub},t,j}$	Adjusted scale frequencies for fish with different fates and unique age/sex class j	
$\text{RLM}_{t,a,s,m}$	Mean length of fish in year t of age a and sex s relative to mesh perimeter m	9

TABLE 3. Prior distributions used for all estimated parameters state-space models. Identical priors were used for all models except where noted by the footnote. Normal distributions were parameterized as (mean, precision) and gamma distributions as (shape, rate) just as in the JAGS language.

Parameter	Prior	Bounds
α	[a]Uniform$(0, X)$	
β	Uniform$(0, 0.5)$	
ϕ	Uniform$(-1, 0.99)$	
$\log(\dot{R}_0)$	Normal$(0, 1 \times 10^{-4})$	
$1/\sigma^2_R$	Gamma$(0.01, 0.01)$	
$1/\sigma^2_{R_0}$	Gamma$(0.01, 0.01)$	
R_y	see eq. (3)	
δ_0	Normal$(0, 1 \times 10^{-6})$	
δ_1	[b]Normal$(0, 1 \times 10^{-6})$	
$\gamma_{0,a,s}$	Normal$(0, 1 \times 10^{-6})$	
$\gamma_{1,a,s}$	[b]Normal$(0, 1 \times 10^{-6})$	
τ	[c]Normal$(1.897, 1/0.46^2)$	
σ	[c]Normal$(0.236, 1/0.81^2)$	[0,∞)
θ	[c]Normal$(0.756, 1/1.86^2)$	[0,∞)
λ	[c]Normal$(-1.049, 1/3.82^2)$	
$F_{\text{com},t}$	Uniform$(0, 10)$	
$F_{\text{sub},t}$	Uniform$(0, 10)$	

Notes

[a] Value of X was 20 for models assuming spawners were the unit of reproductive output (i.e., N-* models) and 0.1 for non-spawner units (i.e., E-* and EM-* models)

[b] In models that assumed time-constant return-by-sex and return-by-age, these priors were replaced with fixed zero values

[c] Estimates provided by N. Smith (ADF&G; methods in Birchfield and Smith 2019), point estimate used as mean, (SE $\times$ 10)^2 used as variance

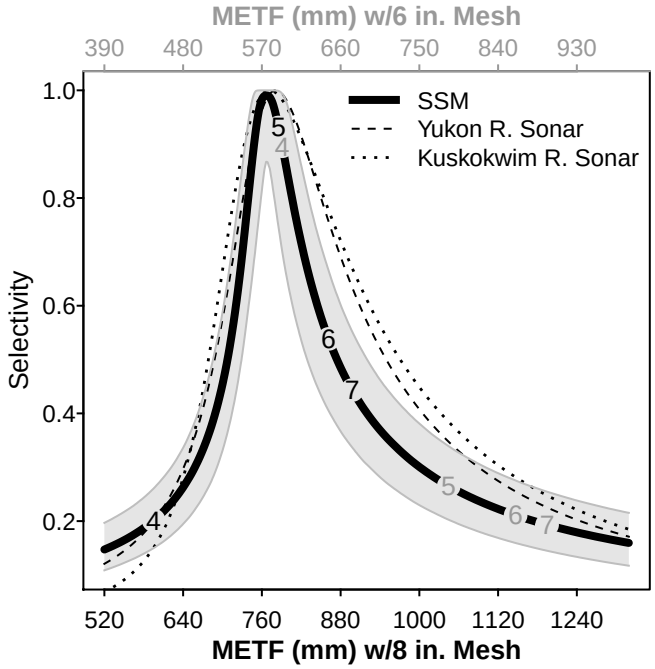

FIGURE 1. Estimated Pearson gillnet selectivity function for Kuskokwim River Chinook salmon. Numbers along the curve indicate the selectivity of females at each age based on the average length across the whole time series according to two mesh sizes: 8-inch (black) and 6-inch (grey). The length (mid-eye to tail-fork; METF) for each mesh size are displayed on the horizontal axes. The grey band represents the 95% credible region for Kuskokwim River Chinook salmon as estimated by the state-space model E-ASL (other models looked identical). For comparative purposes only, Pearson functions are shown for Chinook salmon sampled for sonar-based species apportionment models from the Yukon River (Bromaghin 2005) and Kuskokwim River (N. Smith, personal communication).

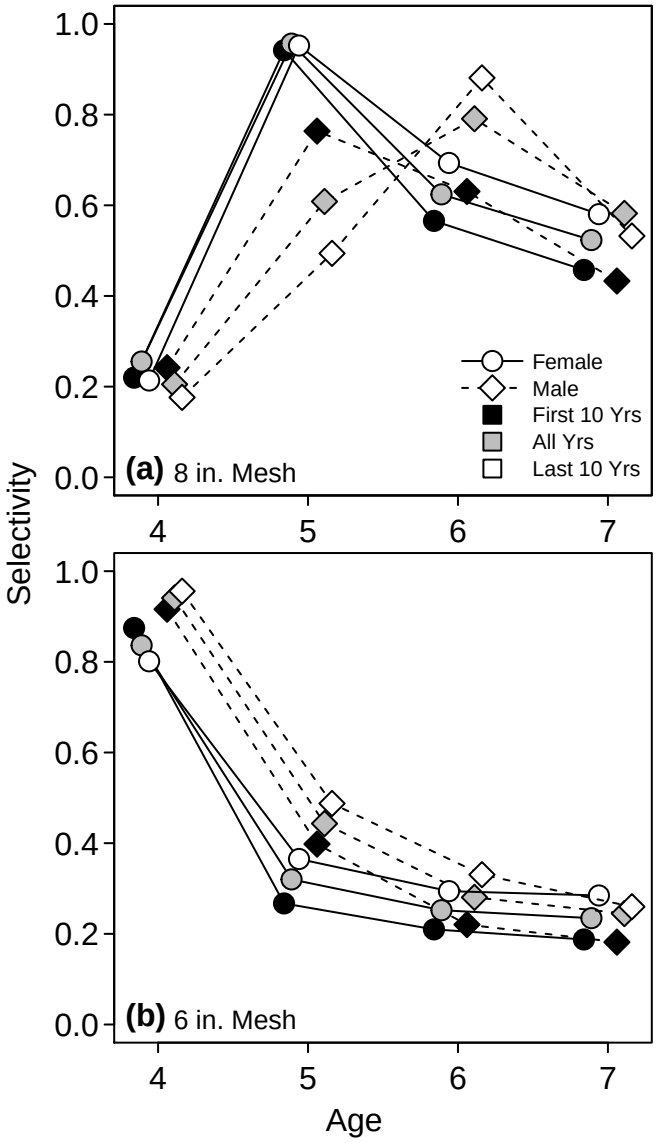

FIGURE 2. Relative selectivity on an age-, sex-, and time period-specific basis for fisheries using (a) 8-inch mesh and (b) 6-inch mesh. Points connected by lines represent the average posterior median for the years included in each time period. Posterior estimates are from model E-ASL; other models looked nearly identical.

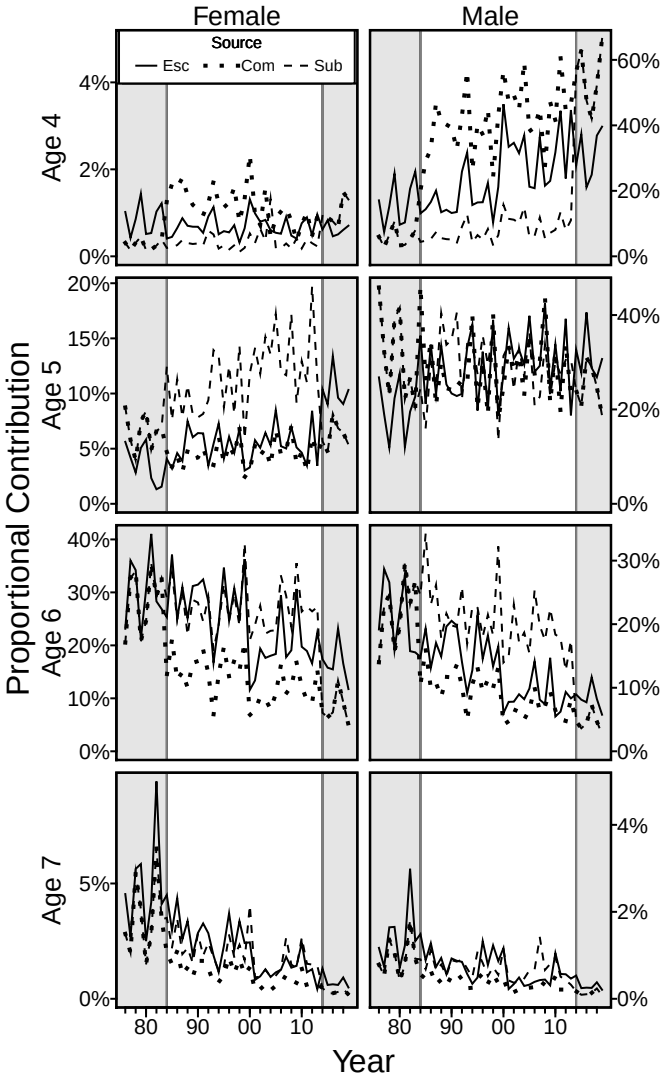

FIGURE 3. Calendar year composition for each age and sex class through time according to three different fates: escapement (solid line), commerical fishery (dotted lines), and subsistence fishery (dashed lines). Lines represent posterior medians from model E-ASL; within a fate and year, all panels sum to one. Grey regions represent the periods when the two fisheries used the same mesh size: 1976 – 1983 both used 8-inch mesh, 1984 – 2011 commercial was restricted to 6-inch mesh, and 2014 – 2019 both were restricted to 6-inch mesh.

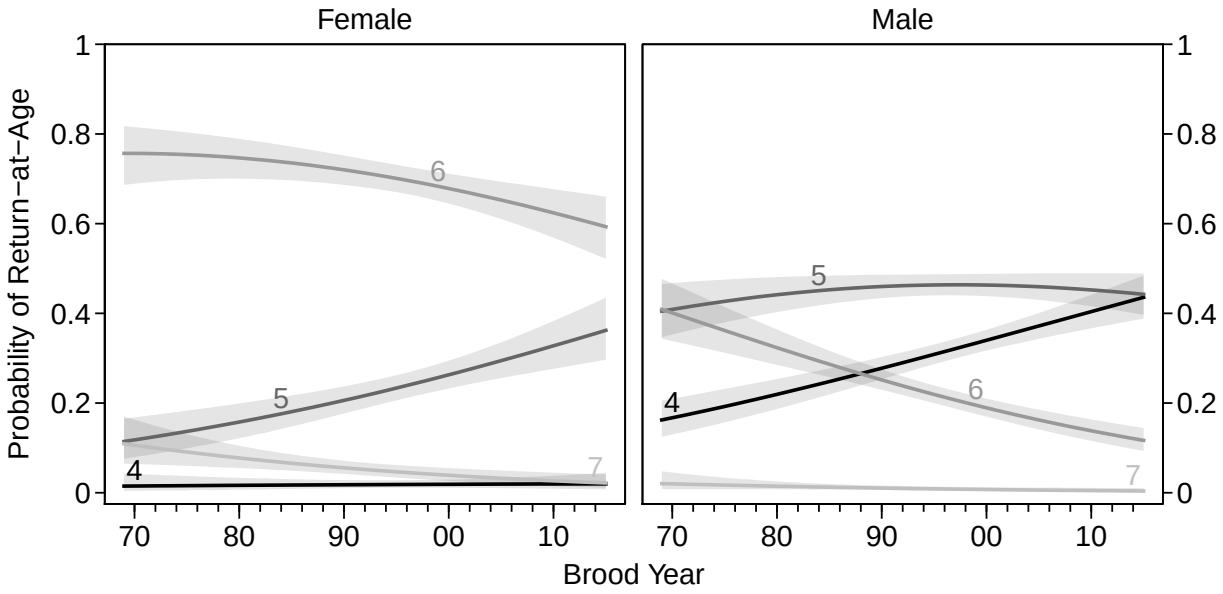

FIGURE 4. Brood year- and sex-specific probability of returning as an adult recruit at each age for models that allowed age-at-return to trend over time (posterior summaries are shown from model E-ASL; but all models with this age component showed the same pattern). The four lines on each panel represent the possible ages of maturity (as indicated by the numerical labels), shaded areas are 95% credible regions, and thick lines are posterior medians. The *x*-axis spans brood years 1969 – 2015.

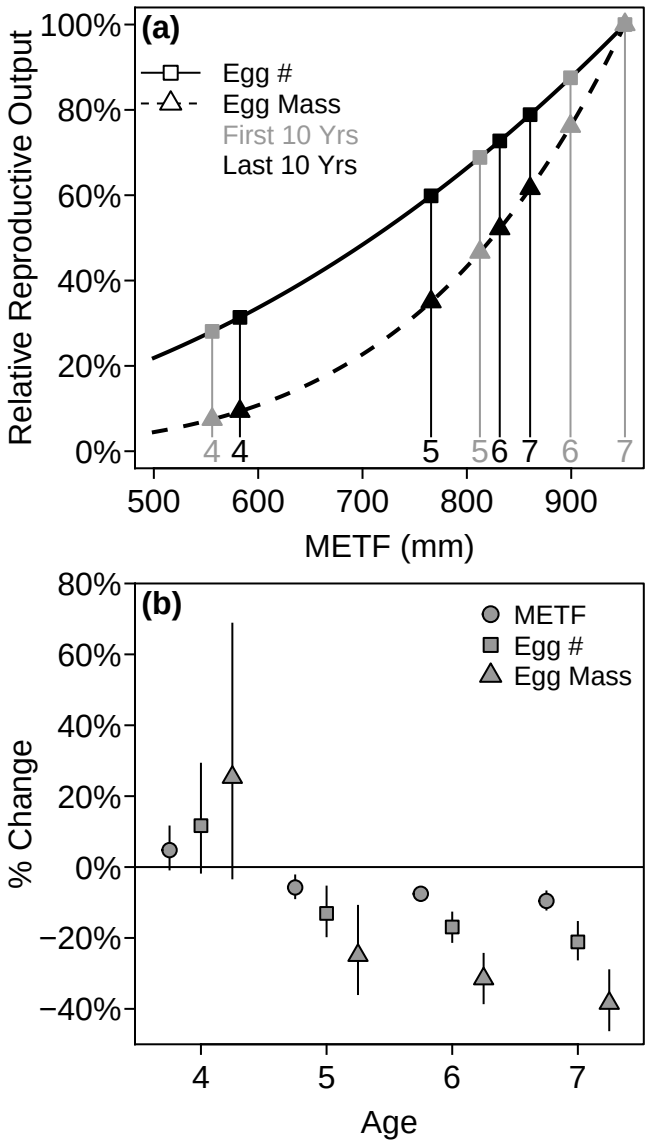

FIGURE 5. Panel (a) shows assumed relationships between female Chinook salmon length (mid-eye to tail-fork; METF) and relative reproductive output expressed as total fecundity (Egg #) or total egg mass per female. Relationships scaled to the reproductive output for age-7 females in the first 10 years of Kuskokwim River mean length data. Numbers and symbols represent METF and relative reproductive output of females at age using METF averaged over the first and last 10 years in the data set. Relationships were fitted to samples taken the Yukon River at Eagle, Alaska between 2008 – 2010 (Ohlberger et al. 2020). Panel (b) shows percent change in METF, egg number, and egg mass per average female spawner of each age between the last and first 10 years of the Kuskokwim data set. Error bars represent 95% bootstrapped confidence limits, obtained by resampling with replacement the mean length values for the years in each time block. Note that although age-4 females are predicted to have increased in size and reproductive output, they make up less than 5% of total female recruits (Figure 4).

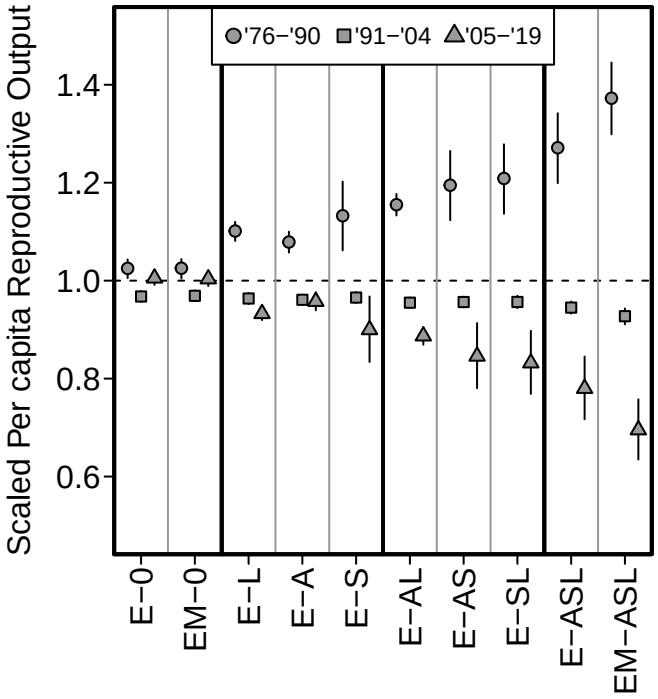

FIGURE 6. Posterior per capita reproductive output (Z_t / S_t, scaled to the mean across all years) averaged for three time periods for each model in the analysis (excluding models N-0 and N-ASL). Larger shifts from the early period (circles) to the later period (triangles) indicate steeper suggested declines in the reproductive output of the average spawner. Points represent posterior medians and error bars represent central 95% credible limits. This measure integrates over age and sex composition while taking into account relative reproductive output.

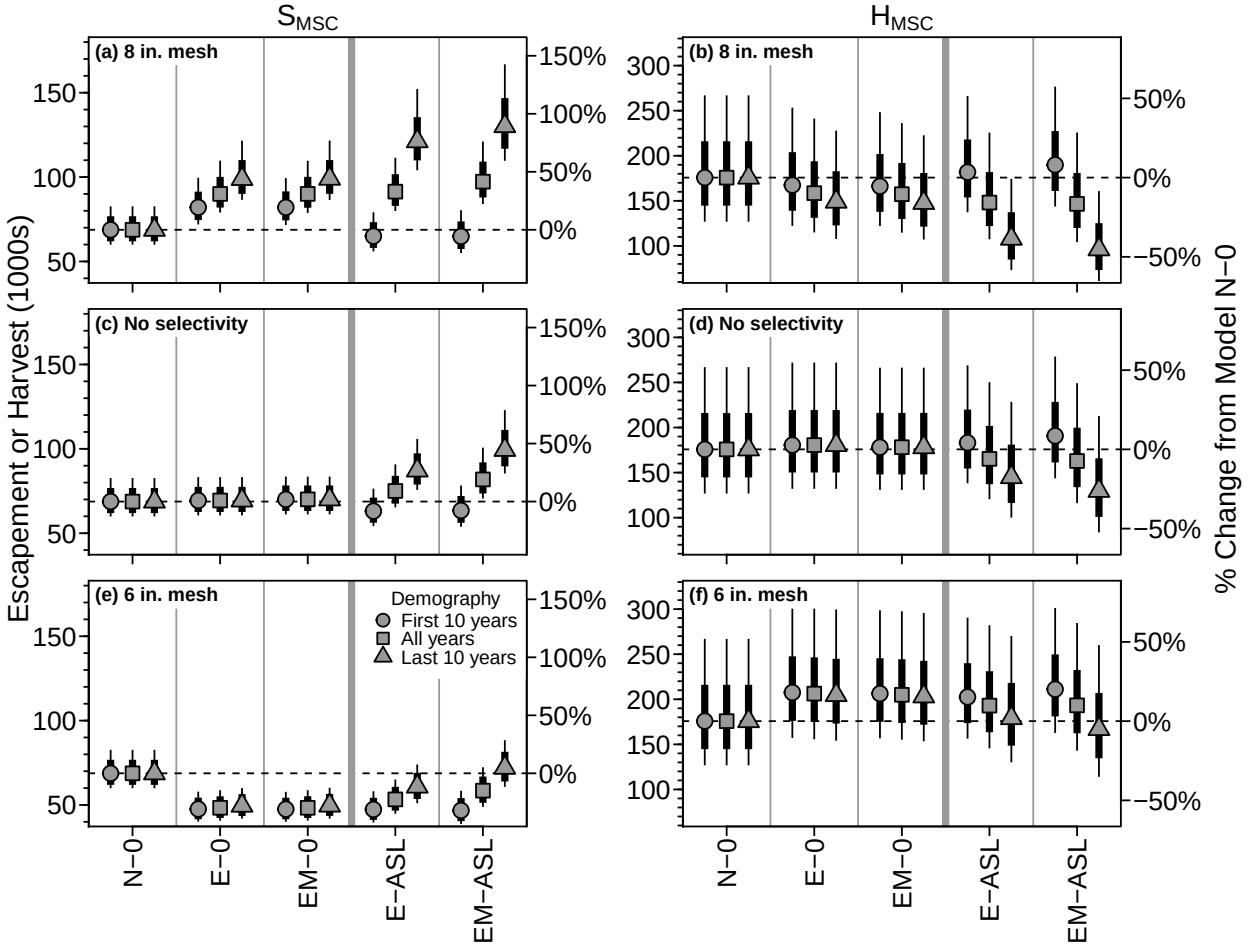

FIGURE 7. Estimated equilibrium values of S_{MSC} (panels a, c, and e) and H_{MSC} (panels b, d, and f) using 8-inch mesh (panels a and b), non-selective (panels c and d), and 6-inch mesh (panels e and f) gillnet gear for a subset of models. The time period (symbol type) represents which years were used to calculate the average demographic qualities used in equilibrium calculations. The percent change from the posterior median for model N-0 is displayed on the secondary *y*-axis for reference. Points are posterior medians, thick lines are the posterior central 50% limits, and thin lines are the posterior central 80% limits.